NJC

PAPER

View Article Online
View Journal | View Issue

Cite this: *New J. Chem.*, 2016, 40, 8872

AuNp@MOF composite as electrochemical material for determination of bisphenol A and its oxidation behavior study†

Cleiser Thiago Pereira da Silva,[a] Fernanda Reis Veregue,[a] Laís Weber Aguiar,[a] Joziane Gimenes Meneguin,[a] Murilo Pereira Moisés,[ab] Silvia Luciana Fávaro,[a] Eduardo Radovanovic,[a] Emerson Marcelo Girotto[a] and Andrelson Wellington Rinaldi*[a]

Received (in Montpellier, France) 24th March 2016,
Accepted 31st August 2016

DOI: 10.1039/c6nj00936k

www.rsc.org/njc

A composite material based on a metal organic framework (MOF), nanowhisker of Al_2O_3 silanized with (3-aminopropyl)triethoxysilane (APTES) and gold nanoparticles (AuNp) was synthesized and characterized. This material was used to prepare an electrode based in carbon paste (CPE) and applied as a sensor for the determination of bisphenol A (BPA). The electrochemical characterizations and behaviour of the electrode containing the AuNp@MOF composite exhibited a 2.3 higher electroactive surface area, when compared with just CPE. Using differential pulse voltammetry (DPV), it can be noted that the presence of AuNp plays an important role in enhancing the analyte signal detection of BPA 2.5-fold. A linear increase in emphasizing the response as a function of analyte concentration is demonstrated. In this account, we believe that this composite may be applied in analyticals methods for the determination of BPA and others endocrine disruptors.

1. Introduction

The monomer bisphenol A (BPA) is a synthetic compound commonly produced and used to synthesize polymers, such as epoxy resins and polycarbonates. These polymers are used in the production of numerous different products, such as CD/DVDs, food packages, bottles, toys, dental products and others.[1,2]

BPA is known as an endocrine disruptor and has been linked to all sorts of health concerns, including cancer development and reproduction problems.[3–6] Although BPA presented low solubility in water (300 mg L^{-1} [7]), it is commonly found in rivers and lakes and it is considered to be an environmental contaminant. Therefore, many efforts have been made to develop an efficient method with high specificity, high sensitivity and low cost for the easy detection of BPA.

Currently, chromatography methods such as gas chromatography (GC) and liquid chromatography (LC) alongside other detections techniques are the most commonly employed methods for the detection of BPA.[8–11] However, these methods require sample preparation and have a relatively high cost. On the other hand, electrochemical sensors have been shown to be an important tool[12–18] to detect BPA by oxidation. Because they have high sensitivity, low response time and the measurements can be conducted without complicated treatment of the samples. In addition, they are cheap, reliable, can be miniaturized and have the potential to be applied to probe environments, such as rivers and lakes, by on line mode. Metal organic frameworks (MOFs) are porous materials with high specific reach up to *ca.* 6000 m^2 g area and usually used to capture gases such as CO_2, N_2, H_2.[19] Some researchers have used MOF to detect substances, such as organic gases,[20] hydrazine,[21] metals,[22] L-cysteine,[23] H_2O_2,[24] glutathione,[25] TNT,[26] humidity,[27] CO_2[28] and BPA.[29] MOFs with gold nanoparticles (AuNp) are used as a sensor to determine hydrazine[21] and L-cysteine.[23] Gold nanoparticles increase the electroactivity and consequently, improve the sensor sensitivity and efficiency. Wang *et al.*[29] used copper with biomolecules of tyrosine immobilized inside of MOF to improve the determination of BPA. Thus, the main goal of this study is to use MOFs loaded with AuNp as electrochemical sensors to determine BPA and study their electrochemical oxidation behavior. We selected carbon paste graphite (CPE) as a platform sensor for our experiments. CPE is composed of carbon graphite powder and a binder (or ligand), *i.e.*, paraffin, mineral oil and others. The main advantages of CPE are low cost, simple manufacture, stability, renewable surface, stable response and sensitivity. Since CPE is the most

[a] *Materials Chemistry and Sensors Laboratory – LMSen, Chemistry Department, State University of Maringá – UEM, Av. Colombo 5790, CEP. 87020-900, Maringá, PR, Brazil. E-mail: andrelson.rinaldi@gmail.com; Fax: +55-443011-4125; Tel: +55-443011-5098*

[b] *Federal University of Technology of Paraná-UTFPR, Rua Marcílio Dias, 635, CEP. 86812-460, Apucarana, PR, Brazil*

† Electronic supplementary information (ESI) available. See DOI: 10.1039/c6nj00936k

used electrode in electrochemistry, many researchers have made modifications to CPE with materials such as Fe_2O_3, carbon nanotubes, cyclodextrins and zeolites.

2. Experimental

2.1. Chemicals and reagents

All the reagents, including bisphenol A (Sigma-Aldrich, 97%), benzene-1,3,5-tricarboxylic acid, TMA (Sigma-Aldrich, 98%), copper(II) nitrate (Vetec, 98%), ethanol (Sigma-Aldrich, 99.5%), phosphoric acid (Synth, 85%), potassium hydroxide (Vetec, 98%), ascorbic acid (Sigma-Aldrich, 99.99%), dimethylformamide – DMF (Vetec, 98%), toluene (Tedia, 99%), aluminum oxide nanopowder – Al_2O_3 nanowires (whiskers), diam. × *L* 2–6 nm × 200–400 nm (Sigma-Aldrich), (3-aminopropyl)triethoxysilane – APTES (Sigma-Aldrich, ≥98%), gold chloride – $HAuCl_4$ solution (Sigma-Aldrich, 99.99%), dichloromethane – $CHCl_2$ (Tedia, 99%), graphite powder synthetic (<20 μm, Sigma-Aldrich), potassium ferricyanide – $K_4[Fe(CN)_6]$ (Vetec, 99%), were of analytical grade purity.

2.2. Nanowhisker APTES silanization

The nanowhiskers were functionalized with APTES by a modified method according to the report in the literature.[30] In brief, 4.0 g of Al_2O_3 nanowhiskers were treated with 4.0 mL of APTES in 140 mL toluene in a bath reflux for 24 h. The nanowhiskers covered with APTES on the surface were centrifuged at 4500 rpm for 30 min, washed with ethanol and dried at 80 °C overnight.

2.3. MOF composite synthesis

The MOF composite material was synthesized by a modified method according to the literature.[31] 2.0 g TMA, 4.0 g copper(II) nitrate and 0.4 g of nanowhiskers-APTES were stirred for 15 min in 100 mL of solvent consisting of equal parts DMF, ethanol and Milli-Q water. Then, this solution was sealed off in a bottle (capacity 150 mL) and placed in an 85 °C oven for 20 h. The products were filtered and washed with DMF and was immersed in dichloromethane for activation.

2.4. AuNp@MOF composite synthesis

The synthesis of AuNp inside of the MOF composite was realized as the following procedure: 100 mg of MOF composite was left in 25 mL of ethanol containing 10 μL of $HAuCl_4$ solution. This suspension was stirred for 2 h, then 2.5 mL of 1% ascorbic acid ethanolic solution was added to the system and left to react for 24 h. After being centrifuged at 4500 rpm for 30 min, washed with ethanol, and dried at 110 °C overnight, the composite material containing AuNp was denominated as AuNp@MOF composite.

2.5. Electrodes preparation

The carbon pastes were prepared by mixing graphite powder, AuNp@MOF composite and four drops of mineral oil. Furthermore, the paste was packed into the cavity (2.5 mm internal diameter and 5 mm depth) of a polypropylene tube with cooper wire as electrical contact. The paste surface was smoothed on a glossy paper at each electrochemical measurement. Different weight ratios (w/w) of graphite powder and AuNp@MOF composite were prepared, 5, 10 and 20 (w/w), in order to test the influence of the amount of composite MOF in the sensor response.

2.6. Electrochemical characterization and measurements

Autolab potentiostat PGSTAT302N was used for electrochemical measurements. In a conventional three electrodes, one-compartment cell consisting of the work carbon paste electrode, a platinum wire counter electrode and a saturated calomel electrode (SCE) was used as the reference electrode. Cyclic voltammetry (CV) experiments were performed using 25 mL of a 5.0×10^{-3} mol L^{-1} $K_4[Fe(CN)_6]$ in 0.1 mol L^{-1} KCl solution over the −0.1 to 0.5 V potential, at room temperature or using 25 mL of 1.0×10^{-3} mol L^{-1} BPA solution in a phosphate buffer (pH 7.0) at 0.020 V s^{-1}. Furthermore, aqueous hydrochloric acid solution (pH 4.0) or aqueous NaOH solution (pH 10.0) at room temperature was employed in CV experiments.

Differential pulse voltammetry (DPV) was used for the detection of BPA in pH 7.0 and the background was recorded in a PBS solution (pH 7.0). Electrochemical study without BPA solution was performed in triplicate and the results shown corresponding to the median (cycle voltammetry).

In the electrochemical study, using BPA, the electrochemical measurements correspond to the first cycle (for both CV cycle and DPV curve); however, the paste surface was smoothed on a glossy paper to perform new measurements.

PXRD analyses were realized with Shimadzu, model XRD-6000 X-ray operated at 40 kV and 40 mA, with Cu Kα as the radiation source, diffraction angle-2θ-in the range of 10°–60°. Scanning electron microscopy (SEM, Shimadzu SSX-550 Superscan) and transmission electron microscopy (TEM, Shimadzu JEOL, JEM 1400, and Image-Pro® PLUS version 4.5.0.29 software) were used for optical characterization. Atomic absorption spectroscopy flame-AAS Analytik Jena ContrAA-300 was performed to calculate the content of gold in the composite. The composite material was digested using *aqua-regia* solution (1 : 3 HNO_3 : HCl).

3. Results and discussion

3.1 Materials characterizations

The design of the AuNp@MOF composite synthesis, Scheme 1, was made with the purpose to explore the large specific area of MOF and it presents considerable electroactivity of AuNp. Previous studies[32] of our research group have shown that AuNp is easily anchored on surfaces that contain amine groups (NH_2) such as APTES. Therefore, we attached the APTES onto the surface of the nanowhiskers with the intention of putting AuNps within the MOF. In addition, the nanoparticles, regardless of metal or oxidation state, can improve the electrochemical properties of materials.[33] Ascorbic acid was used to synthesize AuNp because

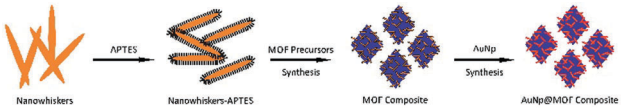

Scheme 1 Synthesis of AuNp@MOF composite synthesis.

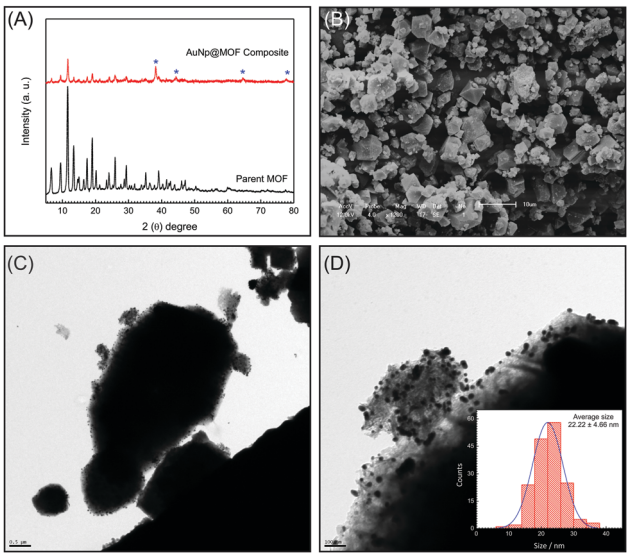

Fig. 1 (A) PXRD and (B) SEM of AuNp@MOF composite. (C and D) TEM of AuNp@MOF composite and average size distribution of AuNp in material (inset) in D.

it is an oxidizing agent weaker than sodium borohydride. The PXRD diffraction peaks for the parent MOF and AuNp@MOF composite are in good agreement with the literature.[31] However, a decrease of crystallinity (80% less) was observed in the PXRD of the AuNp@MOF composite, suggesting that the synthesis procedure might not maintain the structure of the parent MOF intact, Fig. 1(A). Furthermore, the new peaks for the AuNp@MOF composite at 38.22°, 44.34°, 64.52° and 77.70° 2θ match with the gold face cubic center (fcc), in good agreement with the card from Joint Committee on Powder Diffraction Standards (JCPDS, File No. 4-0784). SEM images (Fig. 1(B)) for AuNp@MOF composite looks like an aggregate of materials without definite shape but mixed with some crystals; in other words, the AuNp@MOF composites do not have high crystallinity, as observed in the PXRD diffractogramm. The AuNp is not observed by SEM, however once ascorbic acid is small enough to get through by MOF porous to reduce the Au ions to AuNp we invoked TEM to see this important point. Fig. 1(C and D) show that AuNp are on the surface and as well inside the composite material, as shown in the ESI† Fig. S1. The median size of AuNp calculated is 22.22 ± 4.66 nm (inset. Fig. 1(D)). Lastly, we determined 0.33% as the percentage of gold loaded (w/w) in the MOF matrix by AAS-flame.

3.2 Electrochemical characterizations

With the material in hand, the ratio of 10% (w/w) between the graphite powder and AuNp@MOF composite displayed the best response of the modified CPE, so all electrochemical measurements were realized with this ratio. The CV behaviors of AuNp@MOF composite and MOF composite in 0.1 mol L^{-1} PBS pH 7.0 and 0.1 mol L^{-1} KCl at 20 mV s^{-1} scan rate demonstrated which AuNp@MOF composite have *ca.* 5 times current density larger than the MOF composite. Both the electrodes have one pair of well-defined redox peak wherein the anodic peak potential (E_{pa}) of −0.07 V and a cathodic peak potential of (E_{pc}) −0.19 V

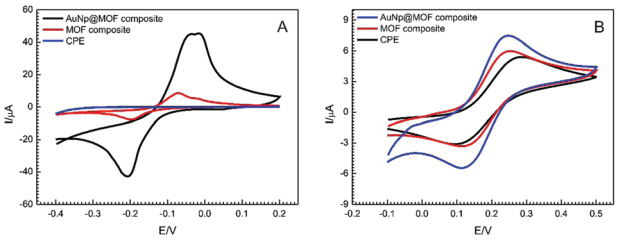

Fig. 2 (A) CV of electrodes in pH 7.0, KCl 0.1 mol L^{-1} and scan rate 20 mV s^{-1}. (B) CV of electrodes in 5.0 mmol L^{-1} of $K_4[Fe(CN)_6]$, KCl 0.1 mol L^{-1} and scan rate 20 mV s^{-1}.

are assigned to the oxidation ($Cu^{I/II}$) and reduction ($Cu^{II/I}$) respectively of the MOF metallic center, as discussed in the literature,[24] Fig. 2(A).

In the presence of $K_4[Fe(CN)_6]$ system (5.0 mmol L^{-1} $K_4[Fe(CN)_6]$ and 0.1 mmol L^{-1} KCl), AuNp@MOF composite and MOF composite show the characteristic pair of redox peaks (oxidation (E_{pa}) and reduction (E_{pc}) of system $[Fe(CN)_6]^{3-/4-}$) (Fig. 2(B)). Although the AuNp@MOF composite showed a slight increase in the density of current, the value found in the difference between E_{pa} and E_{pc} (ΔE_p) for AuNp@MOF composite is 0.134 V, and this value is close to the ΔE_p calculated for MOF composite (0.139 V). However, when we compare this with the ΔE_p calculated for CPE, 0.190 V (AuNp@MOF composite or MOF composite), the difference is significant and this indicates that the decrease of ΔE_p might be caused by the presence of the MOF or the composite in the CPE and not because of the AuNp. Therefore, this encourages us to determine the electroactive surface area of these electrodes using the $K_4[Fe(CN)_6]$ system and the Randles–Sevcik equation, see ESI† and Fig. S2. The electrode with AuNp@MOF composite material has a surface area of 0.167 ± 0.010 cm^2, which is 2.3 times higher compared with the electroactive surface area of CPE (0.072 ± 0.004 cm^2). Thus, we suggest that the synergic effect between AuNp and MOF matrix is responsible for the increase in the density of current. In addition, an additional experiment using gold nanoparticles and CPE does not show a noticeable increase in the current.

The CV of both electrodes in a high concentration solution of BPA (1.0 mmol L^{-1}) shows that the electrodes has electroactivity for BPA oxidation in a solution of pH 7.0. The potential recorded for just CPE (without AuNp@MOF composite or MOF composite) in *ca.* 0.45 V is virtually the same as observed for electrodes with the AuNp@MOF composite and MOF composite. Moreover, CPE and the electrode with MOF composite showed almost the same density of current; the electrode containing AuNp has a notable increased density of current (*ca.* 2.5 times more), (Fig. 3(A)). The CV of electrodes recorded in the same conditions and scan sweeping without BPA does not show any peak of oxidation at or near of 0.45 V (Fig. 3(B)). The anodic potential peak (I_{pa}) of the electrode is affected when BPA undergoes oxidation in the second CV cycle. This occurs because BPA polymerize as thin films on the surface of the electrode, decreasing the density of current. Therefore, we always record the first cycle. Once the electrochemical surface is cleaned with the smooth glassy paper, the electrochemical characteristics of the electrode can be recovered.

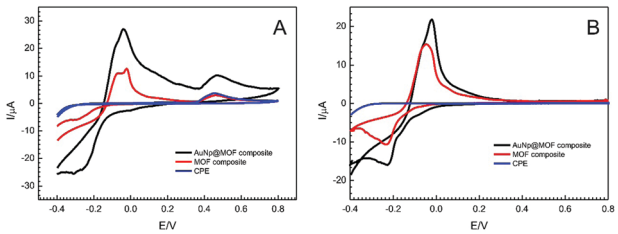

Fig. 3 (A) CV of electrodes in 1 mmol L^{-1} of BPA in pH 7.0, KCl 0.1 mol L^{-1} and scan rate 20 mV s^{-1}. (B) CV without the presence of BPA illustrating the absence of the signal at 450 mV.

3.3 Scan rate and pH effects on the electrode

The electrochemical oxidation behavior of BPA on the AuNp@MOF composite electrode using CV at various scan rates (5–40 mV s^{-1}) is illustrated in Fig. 4(A). We noted that the current peak of BPA oxidation shows a good linear increase with the square root of the scan rate, indicating that the oxidation of BPA is controlled by electron transfer (diffusion-controlled behavior for electrooxidation).[20] The equation obtained is $I = 39.83 \times 10^{-6}$ (V s^{-1}) $- 0.818 \times 10^{-6}$; $R^2 = 0.997$, Fig. 4(B). Moreover, a good linear dependence between the E_{pa} and natural logarithmic of ν ($\ln \nu$ V^{-1} s^{-1}) obeys the Laviron equation[34] (eqn (1)) for a controlled diffusion and irreversible electrochemical process and can be expressed by E_{pa} (V) = 0.020($\ln \nu$) + 0.542, $R^2 = 0.986$, Fig. 4(C).

$$E_{pa} = E^0 + (RT/\alpha nF)\ln(RTk^0/\alpha nF) + (RT/\alpha nF)\ln \nu \qquad (1)$$

E_{pa} is the potential of oxidation of BPA, E^0 is the standard potential, R, T and F have their usual meanings (R = 8.314 J K^{-1} mol^{-1}, T = 298.14 K, and F = 96 480 C), α is the electron transfer coefficient, n is the number of transferred electrons and ν is scan rate. The number of electrons transferred (n) during the oxidation of BPA is obtained from the slope of the curve (value 0.023) in eqn (1). The value for (α) is 0.5 for the irreversible process; the calculated value of (n) was 2.1 which is very close to

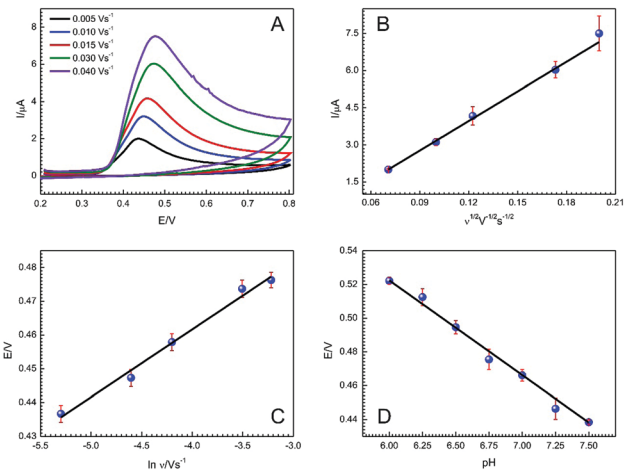

Fig. 4 (A) CV of AuNp@MOF composite in 1 mmol L^{-1} BPA at pH 7.0 in various scan rates; (B) relationship between log I_{pa} *vs.* log E_{pa}; (C) the relationship between the oxidation peak potential (E_{pa}) and $\ln \nu$; (D) relationship of oxidation peak potential of BPA with pH value.

expected value of n = 2 for oxidation of BPA. Subsequently, by CV, the influence of pH on the oxidation of BPA (Fig. S3, ESI†) showed that the redox potential shifts to a negative direction with the increase of pH from 4.0 to 10.0 E_{pa} and pH have a linear relationship, Fig. 4(D).

As described previously,[24] the number of hydrogen ions participating in the reaction of BPA oxidation can be determined through the slope of the curve by the equation – slope $X/n = -0.059$, in which the number X represents H^+. The regression equation is represented by E_{pa} (V) = −0.056 (pH) + 0.859, $R^2 = 0.998$. The slope of curve determined through the slope is 60 mV per pH unit and the number of electrons calculated through the regression equation is 2.1 that is very close of the number of H^+ expected for BPA oxidation, *i.e.*, 2.

3.4 Analytical response for BPA

CV is a powerful technique to study electrochemical reactions; however, in analytical applications, differential pulse voltammetry (DPV) is usually employed because it is more sensitive and efficient. Therefore, we employed DPV in the analysis and detection of BPA. Fig. 5 shows that the electrode AuNp@MOF composite had a greater density of current in the oxidation of BPA. Clearly, AuNp enhanced the density of current by *ca.* 80% and as mentioned above, this occurs due to the excellent electrocatalytic activity of AuNp.

Before applying our electrode in BPA determination, we analyzed the effects of accumulation potential and accumulation time in the oxidation process, but there is no significant effect. In fact, for accumulation potential above 0.0 V, we noted a decrease of performance of the AuNp@MOF composite. This occurs because in positive potentials, the metal organic frameworks become degraded, causing a decrease of the oxidation current peak.

The electrode exhibited a linear correlation between the current peak and the BPA solutions (from 200 to 1000 μmol L^{-1}) (Fig. 6(A)) with the linear equation expressed by I (μA) = 0.01698 [BPA] − 0.8191×10^{-6}, (Fig. 6(B)). The limit of detection, 37.80 μmol L^{-1}, and quantification, 126 μmol L^{-1}, were calculated according to the expressions $3S_b/m$ and $10S_b/m$ (where S_b is the standard deviation of the blank signal and m is the slope of the calibration graph). To evaluate the performance of our electrode sensor in analytical applications, we performed the determination of BPA in distilled water and a recovery of *ca.* 97% of the prepared solution was obtained. Compared to the literature, our sensor has

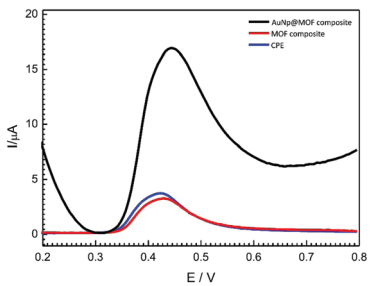

Fig. 5 DPV of electrodes in 1 mmol L^{-1} of BPA in pH 7.0, KCl 0.1 mol L^{-1} and scan rate 20 mV s^{-1}.

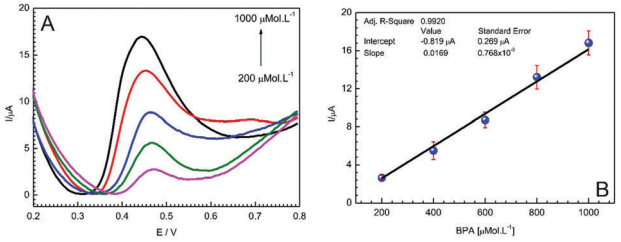

Fig. 6 (A) Potential variation as a function of the concentration of BPA. (B) Response variation as a function of the concentration of BPA, with a linear equation.

a high limit of detection and quantification. However, their applications are quick and easy. This is due the use of CPE electrodes and a physical mix of composite materials plus graphite powder as a part of AuNp@MOF composite. The SEM of the surface of the AuNp@MOF composite electrode, ESI,† Fig. S4, suggests that the surface of CPE is not uniform, which means that most part the composite is inside the CPE and therefore, the porosity of the material is not available to detect the BPA molecules. However, CPE play an important role as a protection against the solution, avoiding MOF degradation. The increase of density of current observed on the electrode containing AuNp@MOF composite indicates that the material is an excellent candidate towards detection or oxidation of BPA. The simplicity and low cost of the electrodes and composite confirm that this may be applied in routine laboratory tests. Furthermore, some other experiments should be performed, or other platforms could be used in attempts to improve the quantification and detection limit of this sensor. In fact, further analyses are in progress in our laboratories. To the best of our knowledge, this is the first paper in the literature wherein the researchers used MOF to determine BPA using MOF and AuNp without an enzyme, see ESI,† Table S1. Therefore, materials and methodologies, which are fast and inexpensive, for the detection of BPA with the intention of providing artifices for monitoring this species in the environment need to be developed. It can be noted that the values detected by the proposed material, even if high values are below the values considered toxic, demonstrated the efficiency and relevance of the material.

4. Conclusions

Taken together, these results demonstrated that we successfully prepared a MOF composite with AuNp inside of the MOF matrix. The composite material used to prepare the CPE electrode exhibited excellent electrooxidation towards BPA. AuNp act synergistically with the MOF improving the electrochemical signal. More experiments should be conducted to improve the signal of this sensor and this is ongoing in our laboratory.

Acknowledgements

The authors thank both the COMCAP–UEM for SEM and TEM analyses and the Brazilian agencies for fellowship CNPQ (Process: 577527/2008-8, 310820/2011-1), Fundação Araucária/PR (Process: 830/2013), and CAPES for financial support.

References

1 J. Michałowicz, *Environ. Toxicol. Pharmacol.*, 2014, **37**, 738–758.
2 N. Olea, R. Pulgar, P. Pérez, F. Olea-Serrano, A. Rivas, A. Novillo-Fertrell, V. Pedraza, A. M. Soto and C. Sonnenschein, *Environ. Health Perspect.*, 1996, **104**, 298–305.
3 C. A. Staples, P. B. Dome, G. M. Klecka, S. T. Oblock and L. R. Harris, *Chemosphere*, 1998, **36**, 2149–2173.
4 J. Z. Brandt, L. T. R. Silveira, T. F. Grassi, J. A. Anselmo-Franci, W. J. Fávaro, S. L. Felisbino, L. F. Barbisan and W. R. Scarano, *Reprod. Toxicol.*, 2014, **43**, 56–66.
5 J. R. Rochester, *Reprod. Toxicol.*, 2013, **42**, 132–155.
6 I. A. Lang, T. S. Galloway, A. Scarlett, W. E. Henley, M. Depledge, R. B. Wallace and D. Melzer, *JAMA, J. Am. Med. Assoc.*, 2008, **300**, 1303–1310.
7 A. Shareef, M. J. Angove, J. D. Wells and B. B. Johnson, *J. Chem. Eng. Data*, 2006, **51**, 879–881.
8 D. D. Azevedo, S. Lacorte, P. V. Barcelo and D. Barcelo, *J. Braz. Chem. Soc.*, 2001, **12**, 532–537.
9 A. G. Asimakopoulos, N. S. Thomaidis and M. A. Koupparis, *Toxicol. Lett.*, 2012, **210**, 141–154.
10 B. Singh, A. Kumar and A. K. Malik, *Crit. Rev. Anal. Chem.*, 2014, **44**, 255–269.
11 H. Nakazawa, Y. Iwasaki and R. Ito, *Anal. Sci.*, 2014, **30**, 25–34.
12 H.-s. Yin, Y.-l. Zhou and S.-y. Ai, *J. Electroanal. Chem.*, 2009, **626**, 80–88.
13 Y. Wang, Y. Yang, L. Xu and J. Zhang, *Electrochim. Acta*, 2011, **56**, 2105–2109.
14 G. F. Pereira, L. S. Andrade, R. C. Rocha-Filho, N. Bocchi and S. R. Biaggio, *Electrochim. Acta*, 2012, **82**, 3–8.
15 F. C. Moraes, I. Cesarino, V. Cesarino, L. H. Mascaro and S. A. S. Machado, *Electrochim. Acta*, 2012, **85**, 560–565.
16 F. C. Moraes, T. A. Silva, I. Cesarino and S. A. S. Machado, *Sens. Actuators, B*, 2013, **177**, 14–18.
17 X. Chen, T. Ren, M. Ma, Z. Wang, G. Zhan and C. Li, *Electrochim. Acta*, 2013, **111**, 49–56.
18 X. Yu, Y. Chen, L. Chang, L. Zhou, F. Tang and X. Wu, *Sens. Actuators, B*, 2013, **186**, 648–656.
19 O. K. Farha, A. O. Yazaydin, I. Eryazici, C. D. Malliakas, B. G. Hauser, M. G. Kanatzidis, S. T. Nguyen, R. Q. Snurr and J. T. Hupp, *Nat. Chem.*, 2010, **2**, 944–948.
20 A. H. Khoshaman and B. Bahreyni, *Sens. Actuators, B*, 2012, **162**, 114–119.
21 H. Hosseini, H. Ahmar, A. Dehghani, A. Bagheri, A. R. Fakhari and M. M. Amini, *Electrochim. Acta*, 2013, **88**, 301–309.
22 Y. Wang, Y. Wu, J. Xie and X. Hu, *Sens. Actuators, B*, 2013, **177**, 1161–1166.
23 H. Hosseini, H. Ahmar, A. Dehghani, A. Bagheri, A. Tadjarodi and A. R. Fakhari, *Biosens. Bioelectron.*, 2013, **42**, 426–429.
24 C. Zhang, M. Wang, L. Liu, X. Yang and X. Xu, *Electrochem. Commun.*, 2013, **33**, 131–134.

25 B. Yuan, R. Zhang, X. Jiao, J. Li, H. Shi and D. Zhang, *Electrochem. Commun.*, 2014, **40**, 92–95.
26 Z. Guo, A. Florea, C. Cristea, F. Bessueille, F. Vocanson, F. Goutaland, A. Zhang, R. Săndulescu, F. Lagarde and N. Jaffrezic-Renault, *Sens. Actuators, B*, 2015, **207**(part B), 960–966.
27 Y. Zhang, B. Fu, K. Liu, Y. Zhang, X. Li, S. Wen, Y. Chen and S. Ruan, *Sens. Actuators, B*, 2014, **201**, 281–285.
28 J. J. Gassensmith, J. Y. Kim, J. M. Holcroft, O. K. Farha, J. F. Stoddart, J. T. Hupp and N. C. Jeong, *J. Am. Chem. Soc.*, 2014, **136**, 8277–8282.
29 X. Wang, X. Lu, L. Wu and J. Chen, *Biosens. Bioelectron.*, 2015, **65**, 295–301.
30 Z. Xie, J. Yang, J. Wang, J. Bai, H. Yin, B. Yuan, J. Lu, Y. Zhang, L. Zhou and C. Duan, *Chem. Commun.*, 2012, **48**, 5977–5979.
31 J. L. C. Rowsell and O. M. Yaghi, *J. Am. Chem. Soc.*, 2006, **128**, 1304–1315.
32 C. T. P. da Silva, J. P. Monteiro, E. Radovanovic and E. M. Girotto, *Sens. Actuators, B*, 2014, **191**, 152–157.
33 C. T. P. da Silva, M. D. d. S. Neto, V. L. Kupfer, S. L. d. Oliveira, N. L. d. C. Domingues and A. W. Rinaldi, *Mater. Lett.*, 2013, **100**, 303–305.
34 G. Xu, L. Gong, H. Dai, X. Li, S. Zhang, S. Lu, Y. Lin, J. Chen, Y. Tong and G. Chen, *Anal. Methods*, 2013, **5**, 3328–3333.